Exp Astron
DOI 10.1007/s10686-009-9170-9

ORIGINAL ARTICLE

Advancing fundamental physics with the Laser Astrometric Test of Relativity

The LATOR mission

S. G. Turyshev · M. Shao · K. L. Nordtvedt · H. Dittus · C. Laemmerzahl · S. Theil · C. Salomon · S. Reynaud · T. Damour · U. Johann · P. Bouyer · P. Touboul · B. Foulon · O. Bertolami · J. Páramos

Received: 12 February 2008 / Accepted: 6 May 2009

S. G. Turyshev · M. Shao
Jet Propulsion Laboratory, California Institute of Technology,
4800 Oak Grove Drive, Pasadena, CA 91109, USA

K. L. Nordtvedt
Northwest Analysis, 118 Sourdough Ridge Road, Bozeman, MT 59715, USA

H. Dittus (✉) · C. Laemmerzahl
Centre of Applied Space Technology & Microgravity (ZARM),
University of Bremen, Am Fallturm, 28359 Bremen, Germany
e-mail: dittus@zarm.uni-bremen.de, hansjoerg.dittus@dlr.de

H. Dittus · S. Theil
Institute of Space Systems, German Aerospace Center,
Robert-Hooke-Straße 7, 28359 Bremen, Germany

S. Theil
e-mail: stephan.theil@dlr.de

C. Salomon · S. Reynaud
Laboratoire Kastler Brossel, Université Pierre et Marie Curie,
Campus Jussieu case 74, 75252 Paris, France

T. Damour
Institut des Hautes Etudes Scientifiques, 35, route de Chartres,
91440 Bures-sur-Yvette, France

U. Johann
Department of Science Programs, Earth Observation and Science,
Astrium GmbH, 88039 Friedrichshafen, Germany

P. Bouyer
Laboratoire Charles Fabry de l'Institut d'Optique, Bat 503,
Centre Scientifique, 91403 Orsay CEDEX, France

Published online: 23 May 2009

Abstract The Laser Astrometric Test of Relativity (LATOR) is an experiment designed to test the metric nature of gravitation—a fundamental postulate of the Einstein's general theory of relativity. The key element of LATOR is a geometric redundancy provided by the long-baseline optical interferometry and interplanetary laser ranging. By using a combination of independent time-series of gravitational deflection of light in the immediate proximity to the Sun, along with measurements of the Shapiro time delay on interplanetary scales (to a precision respectively better than 0.1 picoradians and 1 cm), LATOR will significantly improve our knowledge of relativistic gravity and cosmology. The primary mission objective is i) to measure the key post-Newtonian Eddington parameter γ with accuracy of a part in 10^9. $\frac{1}{2}(1-\gamma)$ is a direct measure for presence of a new interaction in gravitational theory, and, in its search, LATOR goes a factor 30,000 beyond the present best result, Cassini's 2003 test. Other mission objectives include: ii) first measurement of gravity's non-linear effects on light to $\sim$0.01% accuracy; including both the traditional Eddington β parameter and also the spatial metric's 2nd order potential contribution (never measured before); iii) direct measurement of the solar quadrupole moment J_2 (currently unavailable) to accuracy of a part in 200 of its expected size of $\simeq 10^{-7}$; iv) direct measurement of the "frame-dragging" effect on light due to the Sun's rotational gravitomagnetic field, to 0.1% accuracy. LATOR's primary measurement pushes to unprecedented accuracy the search for cosmologically relevant scalar-tensor theories of gravity by looking for a remnant scalar field in today's solar system. We discuss the science objectives of the mission, its technology, mission and optical designs, as well as expected performance of this experiment. LATOR will lead to very robust advances in the tests of fundamental physics: this mission could discover a violation or extension of general relativity and/or reveal the presence of an additional long range interaction in the physical law. There are no analogs to LATOR; it is unique and is a natural culmination of solar system gravity experiments.

Keywords Fundamental physics · Tests of general relativity · Scalar-tensor theories · Modified gravity · Interplanetary laser ranging · Optical interferometry · Picometer-class metrology · LATOR

PACS 04.80.-y · 95.10.Eg · 95.55.Pe

P. Touboul · B. Foulon
Physics and Instrumentation Department, ONERA, BP72,
29 ave de la division Leclerc, 92322 Chatillon, France

O. Bertolami · J. Páramos
Instituto Superior Técnico, Departamento de Física, Av. Rovisco Pais, 1,
1049-001 Lisboa, Portugal

1 Introduction

After almost ninety years since general theory of relativity was born, the Einstein's gravitational theory has survived every test. Such longevity, of course, does not mean that this theory is absolutely correct, but it serves to motivate more accurate tests to determine the level of accuracy at which it is violated. General theory of relativity began with its empirical success in 1915 by explaining the anomalous perihelion precession of Mercury's orbit. Shortly thereafter, Eddington's 1919 observations of star lines-of-sight during a solar eclipse confirmed the doubling of the deflection angles predicted by general relativity as compared to Newtonian-like and Equivalence Principle arguments. This test of gravitational deflection of light made general relativity an instant success.

From these beginnings, general theory of relativity has been verified at ever higher accuracy. Thus, microwave ranging to the Viking Lander on Mars yielded a ∼0.2% accuracy in the tests of general relativity [41, 44, 45]. Spacecraft and planetary radar observations reached an accuracy of ∼0.15% [2, 39]. The astrometric observations of quasars on the solar background performed with Very-Long Baseline Interferometry (VLBI) improved the accuracy of the tests of gravity to ∼0.045% [31, 42, 46]. Lunar laser ranging, a continuing legacy of the Apollo program, provided ∼0.011% verification of general relativity via precision measurements of the lunar orbit [57]. Finally, the recent experiments with the Cassini spacecraft improved the accuracy of the tests to ∼0.0023% [8]. (See Section 2 and Fig. 1.) As a result, today general relativity is the standard theory of gravity when astrometry and spacecraft navigation are concerned.

This paper discusses the Laser Astrometric Test of Relativity (LATOR), the space-based experiment that is designed to significantly improve the

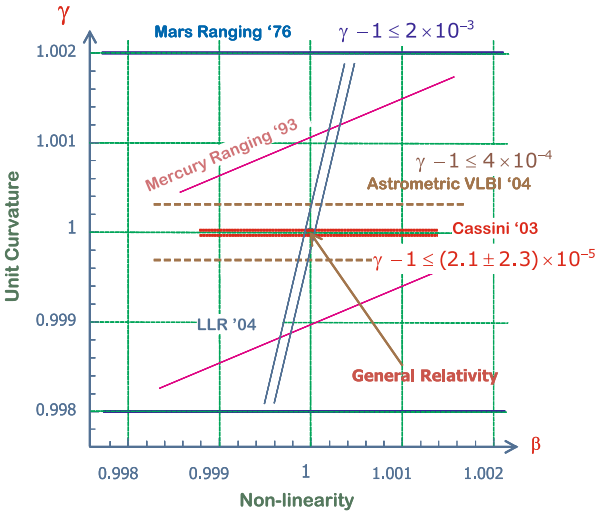

Fig. 1 The progress in improving the knowledge of the PPN parameters γ and β for the last 30 years. So far, general theory of relativity survived every test; however, there are new compelling reasons to continue with the gravitational experiments in the solar system at a significantly improved accuracy

tests of relativistic gravity in the solar system. The primary objective of the LATOR mission will be to measure the gravitational deflection of light by the solar gravity to accuracy of 0.1 picoradians (prad), which corresponds to ∼10 picometers (pm) on a 100 m interferometric baseline. A combination of laser ranging among the spacecraft and direct interferometric measurements will allow LATOR to measure deflection of light in the solar gravity by a factor of ∼30,000 better than had recently been accomplished with the Cassini spacecraft. In particular, LATOR will not only measure the key PPN parameter γ to unprecedented levels of accuracy of one part in 10^9; it will also reach ability to measure the next post-Newtonian order ($\propto G^2$) of light deflection resulting from gravity's intrinsic non-linearity. As a result, LATOR will measure values of other PPN parameters (see Eq. 1) such as parameter δ to 1 part in 10^4 (never measured before), the solar quadrupole moment parameter J_2 to 1 part in 200, and the frame dragging effects on light due to the solar angular momentum to a precision of 1 parts in 10^3.

The paper is organized as follows: Section 2 discusses the theoretical framework and science motivation for the precision gravity tests in the solar system; it also presents the science objectives for the LATOR experiment. Section 3 provides an overview for the LATOR experiment including basic elements of the current mission and optical designs. Section 4 addresses design of the LATOR long-baseline optical interferometer including the laser metrology system. Section 5 discusses the current design for the LATOR flight system and presents a preliminary design for LATOR optical receivers. Section 6 discusses the next steps that will be taken in the development of LATOR.

2 Scientific motivation

Recent remarkable progress in observational cosmology has again submitted general relativity to a test by suggesting a non-Einsteinian model of universe's evolution [38, 43, 54]. From the theoretical standpoint, the challenge is even stronger—if the gravitational field is to be quantized, general relativity will have to be modified. This is why the recent advances in the scalar-tensor extensions of gravity, that are consistent with the current inflationary model of the Big Bang, have motivated new search for a very small deviation of from the Einstein's theory, at the level of accuracy of three to five orders of magnitude below the level tested by experiment.

In this section we will consider the recent theoretical end experimental motivations for the high-accuracy gravitational tests. We will also present the scientific objectives of the LATOR experiment.

2.1 The PPN formalism

Generalizing on a phenomenological parameterization of the gravitational metric tensor field which Eddington originally developed for a special case, a method called the parameterized post-Newtonian (PPN) metric has been

developed [55]. This method represents the gravity tensor's potentials for slowly moving bodies and weak interbody gravity, and it is valid for a broad class of metric theories including general relativity as a unique case. The several parameters in the PPN metric expansion vary from theory to theory, and they are individually associated with various symmetries and invariance properties of underlying theory. Gravity experiments can be analyzed in terms of the PPN metric, and an ensemble of experiments will determine the unique value for these parameters, and hence the metric field, itself.

In locally Lorentz-invariant theories the expansion of the metric field for a single, slowly-rotating gravitational source in PPN coordinates is given by:

$$
\begin{aligned}
g_{00} &= 1 - 2\frac{GM}{c^2 r}\left(1 - J_2\frac{R^2}{r^2}\frac{3\cos^2\theta - 1}{2}\right) + 2\beta\left(\frac{GM}{c^2 r}\right)^2 + \mathcal{O}(c^{-5}),\\
g_{0i} &= 2(\gamma + 1)\frac{G[\mathbf{J}\times\mathbf{r}]_i}{c^3 r^3} + \mathcal{O}(c^{-5}),\\
g_{ij} &= -\delta_{ij}\left[1 + 2\gamma\frac{GM}{c^2 r}\left(1 - J_2\frac{R^2}{r^2}\frac{3\cos^2\theta - 1}{2}\right) + \frac{3}{2}\delta\left(\frac{GM}{c^2 r}\right)^2\right] + \mathcal{O}(c^{-5}),
\end{aligned}
\tag{1}
$$

where M and $\mathbf{J}$ being the mass and angular momentum of the Sun, J_2 being the quadrupole moment of the Sun and R being its radius. r is the distance between the observer and the center of the Sun. β, γ, δ are the PPN parameters and in general relativity they are all equal to 1. The M/r term in the g_{00} equation is the Newtonian limit; the terms multiplied by the post-Newtonian parameters β, γ, are post-Newtonian terms. The term multiplied by the post-post-Newtonian parameter δ also enters the calculation of the relativistic light deflection [34].

This PPN expansion serves as a useful framework to test relativistic gravitation in the context of the LATOR mission. In the special case, when only two PPN parameters (γ, β) are considered, these parameters have clear physical meaning. Parameter γ represents the measure of the curvature of the space-time created by a unit rest mass; parameter β is a measure of the non-linearity of the law of superposition of the gravitational fields in the theory of gravity. General relativity, which corresponds to $\gamma = \beta = 1$, is thus embedded in a two-dimensional space of theories. The Brans-Dicke is the best known theory among the alternative theories of gravity. It contains, besides the metric tensor, a scalar field and an arbitrary coupling constant ω, which yields the two PPN parameter values $\gamma = (1 + \omega)/(2 + \omega)$, and $\beta = 1$. More general scalar tensor theories yield values of β different from one.

2.1.1 Current limits on the PPN parameters γ and β

The PPN formalism has proved to be a versatile method to plan gravitational experiments in the solar system and to analyze the data obtained. Different experiments test different combinations of the PPN parameters (for more details, see [55, 56]). The most precise value for the PPN parameter γ is at present given by the Cassini mission as: $\gamma - 1 = (2.1 \pm 2.3) \times 10^{-5}$ [8]. (Note that the Cassini result constraints the Brans-Dicke scalar coupling constant at

the level of $|\omega| \geq 4.35 \times 10^4$.) The secular trend of Mercury's perihelion, when described in the PPN formalism, depends on another linear combination of the PPN parameters γ and β and the quadrupole coefficient J_2 of the solar gravity field: $\lambda_\odot = (2 + 2\gamma - \beta)/3 + 0.296 \times J_2 \times 10^4$. The combination of parameters $\lambda_\odot$, was obtained with Mercury ranging data as $\lambda_\odot = 0.9996 \pm 0.0006$ [39]. Analysis of planetary ranging data recently yielded an independent determination of parameter γ: $\gamma - 1 = 0.0015 \pm 0.0021$; it also gave β with accuracy at the level of $\beta - 1 = -0.0010 \pm 0.0012$ [1, 2]. The astrometric observations of quasars on the solar background performed with VLBI further reduced the uncertainty in the knowledge of the PPN parameter γ resulting in the limit of $\gamma = 0.99983 \pm 0.00045$ [46].

The PPN formalism has provided a useful framework for testing the violation of the Strong Equivalence Principle (SEP) for gravitationally bound bodies. In that formalism, the ratio of passive gravitational mass M_G to inertial mass M_I of the same body is given by $M_G/M_I = 1 - \eta U_G/(M_0 c^2)$, where M_0 is the rest mass of this body and U_G is the gravitational self-energy. The SEP violation is quantified by the parameter η, which is expressed in terms of the basic set of PPN parameters by the relation $\eta = 4\beta - \gamma - 3$. Additionally, with LLR finding that Earth and Moon fall toward the Sun at rates equal to 1.5 parts in 10^{13}, even in a conservative scenario, where a composition dependence of acceleration rates masks a gravitational self-energy dependence, η is constrained to be less than 0.0008 [1]; without such accidental cancelation the η constraint improves to 0.0003. Using the recent Cassini result [8] on the PPN γ, the parameter β was measured as $\beta - 1 = (0.9 \pm 1.1) \times 10^{-4}$ from LLR [57]. (See Fig. 1.) The next order PPN parameter δ has not yet been measured though its value can be inferred from other measurements.

Over the recent decade, the technology has advanced to the point that one can consider carrying out direct tests in a weak field to the second order in the field strength parameter ($\propto G^2$). Although any measured anomalies in first or second order metric gravity potentials will not determine strong field gravity, they would signal that modifications in the strong field domain will exist. The converse is perhaps more interesting: if to high precision no anomalies are found in the lowest order metric potentials, and this is reinforced by finding no anomalies at the next order, then it follows that any anomalies in the strong gravity environment are correspondingly quenched under all but exceptional circumstances.

2.2 Motivations for precision gravity experiments

The continued inability to merge gravity with quantum mechanics, and recent cosmological observations indicate that the pure tensor gravity of general relativity needs modification. The tensor-scalar theories of gravity, where the usual general relativity tensor field coexists with one or several long-range scalar fields, are believed to be the most promising extension of the theoretical foundation of modern gravitational theory. The superstring, many-dimensional Kaluza-Klein and inflationary cosmology theories have revived

interest in the so-called "dilaton fields," i.e. neutral scalar fields whose background values determine the strength of the coupling constants in the effective four-dimensional theory. The importance of such theories is that they provide a possible route to the quantization of gravity and the unification of physical laws.

Although the scalar fields naturally appear in the theory, their inclusion predicts different relativistic corrections to Newtonian motions in gravitating systems. These deviations from general relativity lead to a violation of the Equivalence Principle (either weak or strong or both), modification of large-scale gravitational phenomena, and generally lead to space and time variation of physical "constants." As a result, this progress has provided new strong motivation for high precision relativistic gravity tests.

2.2.1 Tensor-scalar extensions of general relativity

Recent theoretical findings suggest that the present agreement between general relativity and experiment might be naturally compatible with the existence of a scalar contribution to gravity. In particular, Damour and Nordtvedt [16, 17] (see also [18, 19] for non-metric versions of this mechanism together with [24, 25] for the recent summary of a dilaton-runaway scenario) have found that a scalar-tensor theory of gravity may contain a "built-in" cosmological

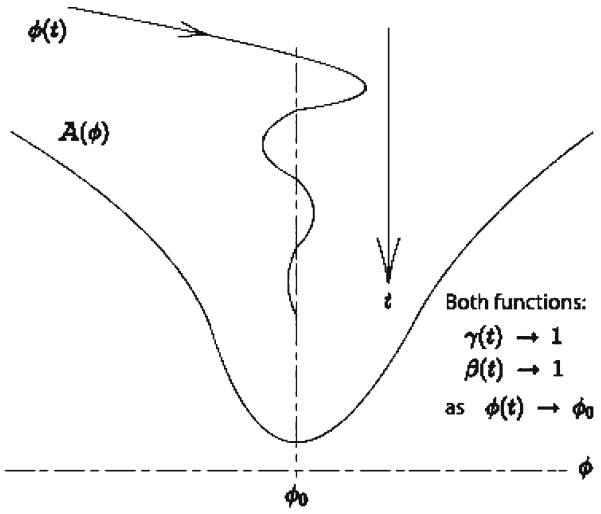

Fig. 2 Typical cosmological dynamics of a background scalar field is shown in the case when that field's coupling function to matter, $V(\phi)$, has an attracting point ϕ_0. The strength of the scalar interaction's coupling to matter is proportional to the derivative (slope) of the coupling function, so it weakens as the attracting point is approached, and both the Eddington parameters γ and β (and all higher structure parameters as well) approach their pure tensor gravity values in this limit. But a small residual scalar gravity should remain today because this dynamical process is not complete, and that is what LATOR experiment seeks to find

attractor mechanism toward general relativity. These scenarios assume that the scalar coupling parameter $\frac{1}{2}(1-\gamma)$ was of order one in the early universe (say, before inflation), and show that it then evolves to be close to, but not exactly equal to, zero at the present time (Fig. 2 illustrates this mechanism in more details).

The Eddington parameter γ, whose value in general relativity is unity, is perhaps the most fundamental PPN parameter, in that $\frac{1}{2}(1-\gamma)$ is a measure, for example, of the fractional strength of the scalar gravity interaction in scalar-tensor theories of gravity [20, 21]. Within perturbation theory for such theories, all other PPN parameters to all relativistic orders collapse to their general relativistic values in proportion to $\frac{1}{2}(1-\gamma)$. This is why measurement of the first order light deflection effect at the level of accuracy comparable with the second-order contribution would provide the crucial information separating alternative scalar-tensor theories of gravity from general relativity [33] and also to probe possible ways for gravity quantization and to test modern theories of cosmological evolution [16–19, 24, 25]. Under some assumptions (see e.g. [16, 17]) one can even estimate what is the likely order of magnitude of the left-over coupling strength at present time which, depending on the total mass density of the universe, can be given as $1-\gamma \sim 7.3\times 10^{-7}(H_0/\Omega_0^3)^{1/2}$, where Ω_0 is the ratio of the current density to the closure density and H_0 is the Hubble constant in units of 100 km/s/Mpc. Compared to the cosmological constant, these scalar field models are consistent with the supernovae observations for a lower matter density, $\Omega_0 \sim 0.2$, and a higher age, $(H_0 t_0) \approx 1$. If this is indeed the case, the level $(1-\gamma) \sim 10^{-6} - 10^{-7}$ would be the lower bound for the present value of PPN parameter γ [16, 17].

More recently, [24, 25] have estimated $\frac{1}{2}(1-\gamma)$, within the framework compatible with string theory and modern cosmology, which basically confirms the previous result [16, 17]. This recent analysis discusses a scenario when a composition-independent coupling of dilaton to hadronic matter produces detectable deviations from general relativity in high-accuracy light deflection experiments in the solar system. This work assumes only some general property of the coupling functions (for large values of the field, i.e. for an "attractor at infinity") and then only assume that $(1-\gamma)$ is of order of one at the beginning of the controllably classical part of inflation. It was shown in [24, 25] that one can relate the present value of $\frac{1}{2}(1-\gamma)$ to the cosmological density fluctuations. For the simplest inflationary potentials (favored by WMAP mission, i.e. $m^2\chi^2$ [4]), [24, 25] found that the present value of $(1-\gamma)$ could be just below 10^{-7}. In particular, within this framework $\frac{1}{2}(1-\gamma) \simeq \alpha_{\rm had}^2$, where $\alpha_{\rm had}$ is the dilaton coupling to hadronic matter; its value depends on the model taken for the inflation potential $V(\chi) \propto \chi^n$, with χ being the inflation field; the level of the expected deviations from general relativity is $\sim 0.5\times 10^{-7}$ for $n=2$ [24, 25]. Note that these predictions are based on the work in scalar-tensor extensions of gravity which are consistent with, and indeed often part of, present cosmological models.

Another example of recent theoretical progress is the Dvali-Gabadadze-Porrati (DGP) brane-world model, which explores a possibility that we live

on a brane embedded in a large extra dimension, and where the strength of gravity in the bulk is substantially less than that on the brane [26]. Although such theories can lead to perfectly conventional gravity on large scales, it is also possible to choose the dynamics in such a way that new effects show up exclusively in the far infrared providing a mechanism to explain the acceleration of the universe [38, 43]. It is interesting to note that DGP gravity and other modifications of GR hold out the possibility of having interesting and testable predictions that distinguish them from models of dynamical Dark Energy. One outcome of this work is that the physics of the accelerating universe may be deeply tied to the properties of gravity on relatively short scales, from millimeters to astronomical units [5, 6, 27, 28].

To date general relativity and some other alternative gravitational theories are in good agreement with the experimental data collected from the relativistic celestial mechanical extremes provided by the relativistic motions in the binary millisecond pulsars. At the same time, many modern theoretical models, which include general relativity as a standard gravity theory, are faced with the problem of the unavoidable appearance of space-time singularities. It is generally suspected that the classical description, provided by general relativity, breaks down in a domain where the curvature is large, and, hence, a proper understanding of such regions requires new physics. This is a reason why recently a considerable interest has been shown in the physical processes occurring in the strong gravitational field regime with relativistic pulsars providing a promising possibility to test gravity in this qualitatively different dynamical environment. The general theoretical framework for pulsar tests of strong-field gravity was introduced in [23]; the observational data for the initial tests were obtained with PSR1534 [47]. An analysis of strong-field gravitational tests and their theoretical justification was presented in [20–22]. The recent analysis of the pulsar data resulted in $\frac{1}{2}(1-\gamma) \simeq \alpha_{\rm had}^2 \sim 4 \times 10^{-4}$ at a 3σ confidence level [30], with $\alpha_{\rm had}$ being the dilaton coupling to hadronic matter. While being a natural alternative to the weak-gravity tests, the pulsar tests of gravitation currently can not offer the accuracy at the level that is presently available within the solar system. In fact, a carefully designed dedicated experiment that utilizes the strongest gravitational potential available in the solar system, provided by the sun itself, offers a unique opportunity to test gravitation in a controlled and the well-understood environment. Therefore, despite the relative weakness of its gravitational field, the sun still has an advantage and offers an attractive opportunity to perform accurate tests of gravity.

The analyses discussed above not only motivate new searches for very small deviations of relativistic gravity in the solar system, they also predict that such deviations are currently present in the range from 10^{-5} to 5×10^{-8} for $\frac{1}{2}(1-\gamma)$, i.e. for observable post-Newtonian deviations from general relativity predictions and, thus, should be easily detectable with LATOR. This would require measurement of the effects of the next post-Newtonian order ($\propto G^2$) of light deflection resulting from gravity's intrinsic non-linearity. An ability to measure the first order light deflection term at the accuracy comparable with

the effects of the second order is of the utmost importance for gravitational theory and a major challenge for the 21st century fundamental physics.

2.2.2 Observational motivations for higher accuracy tests of gravity

Recent astrophysical measurements of the angular structure of the cosmic microwave background [9], the masses of large-scale structures [37], and the luminosity distances of type Ia supernovae [38, 43] have placed stringent constraints on the cosmological constant Λ and also have led to a revolutionary conclusion: the expansion of the universe is accelerating. The implication of these observations for cosmological models is that a classically evolving scalar field currently dominates the energy density of the universe. Such models have been shown to share the advantages of Λ: compatibility with the spatial flatness predicted inflation; a universe older than the standard Einstein-de Sitter model; and, combined with cold dark matter, predictions for large-scale structure formation in good agreement with data from galaxy surveys. Combined with the fact that scalar field models imprint distinctive signature on the cosmic microwave background (CMB) anisotropy, they remain currently viable and should be tested in the near future. This unexpected discovery demonstrates the importance of testing the important ideas about the nature of gravity. We are presently in the "discovery" phase of this new physics, and while there are many theoretical conjectures as to the origin of a non-zero Λ, it is essential that we exploit every available opportunity to elucidate the physics that is at the root of the observed phenomena.

There is now multiple evidence indicating that 70% of the critical density of the universe is in the form of a "negative-pressure" dark energy component; there is no understanding as to its origin and nature. The fact that the expansion of the universe is currently undergoing a period of acceleration now seems rather well tested: it is directly measured from the light-curves of several hundred type Ia supernovae [38, 43, 48], and independently inferred from observations of CMB by the WMAP satellite [4] and other CMB experiments [29, 32]. Cosmic speed-up can be accommodated within general relativity by invoking a mysterious cosmic fluid with large negative pressure, dubbed dark energy. The simplest possibility for dark energy is a cosmological constant; unfortunately, the smallest estimates for its value are 55 orders of magnitude too large [11, 36]. Most of the theoretical studies operate in the shadow of the cosmological constant problem, the most embarrassing hierarchy problem in physics. This fact has motivated a host of other possibilities, most of which assume $\Lambda = 0$, with the dynamical dark energy being associated with a new scalar field (see [13, 14] and references therein). However, none of these suggestions is compelling and most have serious drawbacks.

Given the challenge of this problem, a number of authors considered the possibility that cosmic acceleration is not due to some kind of stuff, but rather arises from new gravitational physics (see discussion in [11–13, 36]). In particular, certain extensions to general relativity in a low energy regime [10, 13, 15] were shown to predict an experimentally consistent universe evolution without

the need for dark energy (see discussion on the interplay between theory, experiment and observation in [3, 7]). These dynamical models are expected to explain the observed acceleration of the universe without dark energy, but may produce measurable gravitational effects on the scales of the solar system. In particular, corresponding contribution to the parameter γ in experiments conducted in the solar system are expected at the level of $1-\gamma \sim 10^{-7} - 5 \times 10^{-9}$, thus further motivating the relativistic gravity research. Therefore, the PPN parameter γ may be the only key parameter that holds the answer to most of the questions discussed above. Also an anomalous parameter δ will most likely be accompanied by a "γ mass" of the Sun which differs from the gravitational mass of the Sun and therefore will show up as anomalous γ (see discussion in [35]).

In summary, there are a number of theoretical and experimental reasons to question the validity of general relativity. Despite the success of modern gauge field theories in describing the electromagnetic, weak, and strong interactions, it is still not understood how gravity should be described at the quantum level. In theories that attempt to include gravity, new long-range forces can arise in addition to the Newtonian inverse-square law. Even at the purely classical level, and assuming the validity of the Equivalence Principle, Einstein's theory does not provide the most general way to generate the space-time metric. The LATOR mission is designed to directly address theses challenges with an unprecedented accuracy; we shall now discuss LATOR in more details.

3 Overview of LATOR

The LATOR experiment uses the standard technique of time-of-fight laser ranging (extended to interplanetary scales) between two micro-spacecraft whose lines of sight pass close by the Sun and also a long-baseline stellar optical interferometer (placed above the Earth's atmosphere) to accurately measure deflection of light by the solar gravitational field in the extreme proximity to the Sun [49]. Figure 3 shows the general concept for the LATOR missions including the mission-related geometry, experiment details and required accuracies.

In this section we will consider the LATOR mission architecture in more detail.

3.1 Evolving light triangle

The LATOR mission architecture uses an evolving light triangle formed by laser ranging between two spacecraft (placed in ~1 AU heliocentric orbits) and a laser transceiver terminal on the International Space Station (ISS) (realized via European collaboration [52]). The objective is to measure the gravitational deflection of laser light as it passes in extreme proximity to the Sun (see Fig. 3). To that extent, the long-baseline (~100 m) fiber-coupled optical interferometer on the ISS will perform differential astrometric measurements

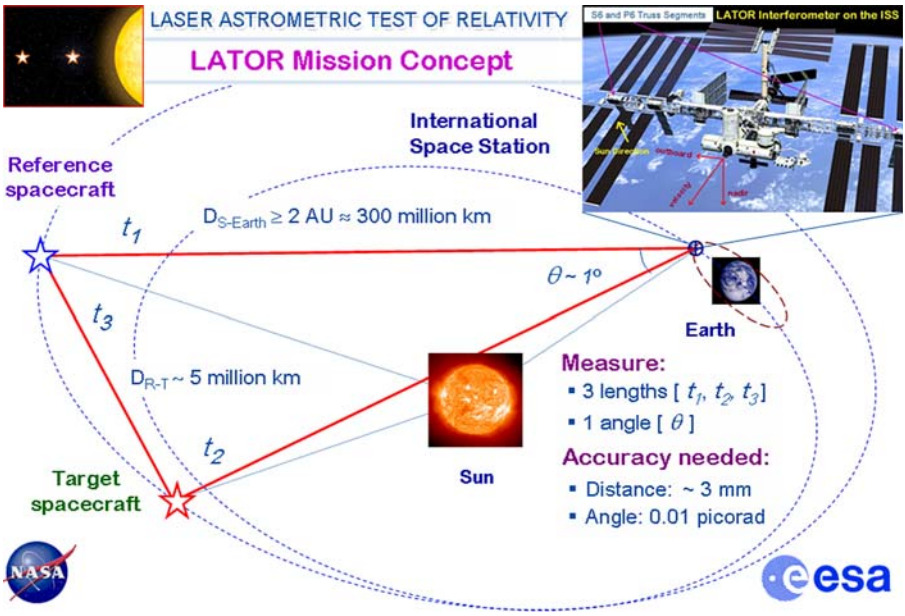

Fig. 3 The overall geometry of the LATOR experiment

of the laser light sources on the two spacecraft as their lines-of-sight pass behind the Sun.

As seen from the Earth, the two spacecraft will be separated by $\sim 1°$, which will be accomplished by a small maneuver immediately after their launch [49, 51]. This separation would permit differential astrometric observations to an accuracy of ~0.1 picorad needed to significantly improve measurements of gravitational deflection of light in the solar gravity.

The schematic of the LATOR experiment is quite simple and is given in Fig. 3. Two spacecraft are injected into a heliocentric solar orbit on the opposite side of the Sun from the Earth. The triangle in the figure has three independent quantities but three arms are monitored with laser metrology. Each spacecraft equipped with a laser ranging system that enables a measurement of the arms of the triangle formed by the two spacecraft and the ISS. The uniqueness of this mission comes with its geometrically redundant architecture that enables LATOR to measure the departure from Euclidean geometry ($\sim 8.48 \times 10^{-6}$ rad) caused by the solar gravity field, to a very high accuracy [49]. This departure is shown as a difference between the calculated Euclidean value for an angle in the triangle and its value directly measured by the interferometer. This discrepancy, which results from the curvature of the space-time around the Sun and can be computed for every alternative theory of gravity, constitutes LATOR's signal of interest. The precise measurement of this departure constitutes the primary mission objective.

3.2 General approach in optical design

A single aperture of the interferometer on the ISS consists of three 30 cm diameter telescopes (see Fig. 4 for a conceptual design). One of the telescopes with a very narrow bandwidth laser line filter in front and with an InGaAs camera at its focal plane, sensitive to the 1064 nm laser light, serves as the acquisition telescope to locate the spacecraft near the Sun.

The second telescope emits the directing beacon to the spacecraft. Both spacecraft are served out of one telescope by a pair of piezo controlled mirrors placed on the focal plane. The properly collimated laser light (1 W) is injected into the telescope focal plane and deflected in the right direction by the piezo-actuated mirrors.

The third telescope is the laser light tracking interferometer input aperture, which can track both spacecraft at the same time. To eliminate beam walk on the critical elements of this telescope, two piezo-electric X-Y-Z stages are used to move two single-mode fiber tips on a spherical surface while maintaining focus and beam position on the fibers and other optics. Dithering at a few Hz is used to make the alignment to the fibers and the subsequent tracking of the two spacecraft completely automatic. The interferometric tracking telescopes are coupled together by a network of single-mode fibers whose relative length

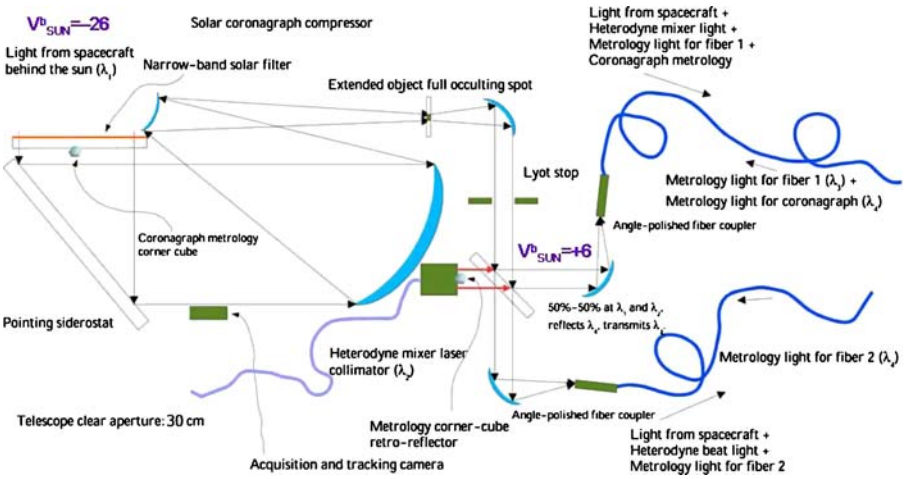

Fig. 4 Basic elements of optical design for the LATOR interferometer: The laser light (together with the solar background) is going through a full aperture (~ 30 cm) narrow band-pass filter with 5×10^{-5} μm bandwidth around wavelength of $\lambda = 1064$ nm. The remaining light illuminates the baseline metrology corner cube and falls onto a steering flat mirror where it is reflected to an off-axis telescope with no central obscuration (needed for metrology). It then enters the solar coronograph compressor (with 1×10^{-5} suppression properties) by first going through a 1/2 plane focal plane occulter and then coming to a Lyot stop. At the Lyot stop, the background solar light is reduced by a factor of 10^6. This combination of a narrow band-pass filter and coronograph enables the solar luminosity reduction from $V = -26$ to $V = 4$, thus enabling the LATOR precision observations

changes are measured internally by a heterodyne metrology system to an accuracy of less than 5 pm.

The spacecraft are identical in construction and contain a relatively high powered (1 W), stable (2 MHz per hour ~500 Hz per second), small cavity fiber-amplified laser at 1064 nm. The power of this laser is directed to the Earth through a 20 cm aperture telescope and its phase is tracked by the interferometer. With the available power and the beam divergence, there are enough photons to track the slowly drifting phase of the laser light. There is another 0.2 W laser operating at 780 nm, the power of which is transmitted through another telescope with small aperture of 5 cm, which points toward the other spacecraft. In addition to the two transmitting telescopes, each spacecraft has two receiving telescopes. The receiving telescope, which points toward the area near the Sun, has laser line filters and a simple knife-edge coronagraph to suppress the Sun's light to 1 part in 10^5 of the light level of the light received from the space station. The receiving telescope that points to the other spacecraft is free of the Sun light filter and the coronagraph.

In addition to the four telescopes they carry, the spacecraft also carry a tiny (2.5 cm) telescope with a CCD camera. This telescope is used to initially point the spacecraft directly toward the Sun so that their signal may be seen at the space station. One more of these small telescopes may also be installed at right angles to the first one, to determine the spacecraft attitude, using known, bright stars. The receiving telescope looking toward the other spacecraft may be used for this purpose part of the time, reducing hardware complexity. Star trackers with this construction were demonstrated many years ago and they are readily available. A small RF transponder with an omni-directional antenna is also included in the instrument package to track the spacecraft while they are on their way to assume the orbital position needed for the experiment.

The LATOR experiment has a number of advantages over techniques that use radio waves to measure gravitational light deflection. Advances in optical communications technology, allow low bandwidth telecommunications with the LATOR spacecraft without having to deploy high gain radio antennae needed to communicate through the solar corona. The use of the monochromatic light enables the observation of the spacecraft almost at the limb of the Sun, as seen from the ISS. The use of narrowband filters, coronagraph optics and heterodyne detection will suppress background light to a level where the solar background is no longer the dominant noise source. In addition, the short wavelength allows much more efficient links with smaller apertures, thereby eliminating the need for a deployable antenna. Finally, the use of the ISS will allow conducting the test above the Earth's atmosphere—the major source of astrometric noise for any ground based interferometer. This fact justifies LATOR as a space mission.

3.3 Science objectives

LATOR is a Michelson-Morley-type experiment designed to test the pure tensor metric nature of gravitation—a fundamental postulate of Einstein's

theory of general relativity [49]. With its focus on gravity's action on light propagation it complements other tests which rely on the gravitational dynamics of bodies. The idea behind this experiment is to use a combination of independent time-series of highly accurate measurements of the gravitational deflection of light in the immediate proximity to the Sun along with measurements of the Shapiro time delay on the interplanetary scales (to a precision respectively better than 0.1 prad and 1 cm). Such a combination of observables is unique and enables LATOR to significantly improve tests of relativistic gravity.

The LATOR's primary mission objective is to measure the key post-Newtonian Eddington parameter γ with an accuracy of a part in 10^9. When the light deflection in solar gravity is concerned, the magnitude of the first order effect as predicted by general relativity for the light ray just grazing the limb of the Sun is ~ 1.75 arcsecond (asec) (for more details see Table 1). (Note that 1 arcsec $\simeq 5$ μrad; when convenient, below we will use the units of radians and arcseconds interchangeably.) The effect varies inversely with the impact parameter. The second order term is almost six orders of magnitude smaller resulting in ~ 3.5 microarcseconds (μas) light deflection effect, and which falls off inversely as the square of the light ray's impact parameter [33, 49]. The relativistic frame-dragging term is ± 0.7 μas, and contribution of the solar quadrupole moment, J_2, is sized as 0.2 μas (using theoretical value of the solar quadrupole moment $J_2 \simeq 10^{-7}$). The small magnitudes of the effects emphasize the fact that, among the four forces of nature, gravitation is the weakest interaction; it acts at very long distances and controls the large-scale structure of the universe, thus, making the precision tests of gravity a very challenging task.

If the Eddington's 1919 experiment was performed to confirm general relativity, LATOR is motivated to search for physics beyond the Einstein's theory of gravity with an unprecedented accuracy [49]. In fact, this mission is designed to address the questions of fundamental importance to modern physics. In particular, this solar system scale experiment would search for a cosmologically-evolved scalar field that is predicted by modern theories of quantum gravity and cosmology, and also by superstring and brane-world models [5–7, 26]. LATOR will also test the cosmologically motivated theories that attempt to explain the small acceleration rate of the Universe (so-called

Table 1 Comparable sizes of various light deflection effects in the solar gravity field

Effect	Analytic form	Deflection angle, μas	Delay for $b = 100$ m, pm
First order	$2(1+\gamma)\frac{M}{p}$	1.75 arcsec	0.849 mm
Second order	$[(2(1+\gamma)-\beta+\frac{3}{4}\delta)\pi - 2(1+\gamma)^2]\frac{M^2}{p^2}$	3.5	1697
Frame-dragging	$\pm 2(1+\gamma)\frac{J}{p^2}$	± 0.7	± 339
Solar quadrupole	$2(1+\gamma)J_2\frac{M}{p^3}$	0.2	97

The value of deflection angle is calculated on the limb of the Sun ($p = R_\odot$); the corresponding delay is given for a $b = 100$ m interferometric baseline proposed for LATOR

Table 2 LATOR mission summary: science objectives

Qualitative objectives:

- To test the metric nature of the Einstein's general theory of relativity in the most intense gravitational environment available in the solar system – the extreme proximity to the Sun;
- To test alternative theories of gravity and cosmology, notably scalar-tensor theories, by searching for cosmological remnants of scalar field in the solar system;
- To verify the models of light propagation and motion of the gravitationally-bounded systems at the second post-Newtonian order (i.e. including effects $\propto G^2$).

Quantitative objectives:

- To measure the key Eddington PPN parameter γ with accuracy of 1 part in 10^9—a factor of 30,000 improvement in the tests of gravitational deflection of light;
- To provide direct and independent measurement of the Eddington PPN parameter β via gravity effect on light to $\sim 0.01\%$ accuracy;
- To measure effect of the 2-nd order gravitational deflection of light with accuracy of 1 part in 10^4, including first ever measurement of the post-PPN parameter δ;
- To directly measure the frame dragging effect on light (first such observation and also first direct measurement of solar spin) with accuracy of 1 part in 10^3;
- To measure the solar quadrupole moment J_2 (using the theoretical value of $J_2 \simeq 10^{-7}$, currently unavailable) to 1 part in 200.

"dark energy") via modification of gravity at very large, horizon or super-horizon distances.

By studying the effect of gravity on light and measuring the Eddington parameter γ, this mission will tests the presently viable alternative theories of gravity, namely the scalar-tensor theories. The value of the parameter γ may hold the key to the solution of the most fundamental questions concerning the evolution of the universe. In the low energy approximation suitable for the solar system, a number of modern theories of gravity and cosmology studied as methods for gravity quantization or proposed as an explanation to the recent cosmological puzzles, predict measurable contributions to the parameter γ at the level of $\frac{1}{2}(1-\gamma) \sim 10^{-6} - 10^{-8}$; detecting this deviation is LATOR's primary objective. With the accuracy of one part in 10^9, this mission could discover a violation or extension of general relativity, and/or reveal the presence of any additional long range interaction (Table 2).

3.4 Spacecraft trajectory: a 3:2 earth resonant orbit

To enable the primary objective, LATOR will place two spacecraft into a heliocentric orbit, to provide conditions for observing the spacecraft when they are behind the Sun as viewed from the ISS (see Figs. 5, 6). We analyzed various trajectory options for the deep-space flight segment of LATOR, using standard JPL navigation software packages.

An orbit with a 3:2 resonance with the Earth was found to uniquely satisfy the LATOR orbital requirements [49]. For this orbit, 13 months after the launch, the spacecraft are within $\sim 10^\circ$ of the Sun with first occultation

occurring 15 months after launch [49]. At this point, LATOR is orbiting at a slower speed than the Earth, but as LATOR approaches its perihelion, its motion in the sky begins to reverse and the spacecraft is again occulted by the Sun 18 months after launch. As the spacecraft slows down and moves out toward aphelion, its motion in the sky reverses again, and it is occulted by the Sun for the third and final time 21 months after launch.

This entire process will again repeat itself in about 3 years after the initial occultation, however, there may be a small maneuver required to allow for more occultations. Therefore, to allow for more occultations in the future, there may be a need for an extra few tens of m/s of Δv. The energy required for launch, C_3, will vary between $\sim (10.6 - 11.4)$ km^2/s^2 depending on the time of launch, but it is suitable for a Delta II launch vehicle. The desirable $\sim 1^\circ$ spacecraft separation (as seen from the Earth) is achieved by performing a 30 m/s maneuver after the launch. This results in the second spacecraft being within $\sim (0.6 - 1.4)^\circ$ separation during the entire period of 3 occultations by the Sun.

Figure 5 shows the trajectory and the occultations in more details. The figure on the right is the spacecraft position in the solar system showing the Earth's and LATOR's orbits (in the 3:2 resonance) relative to the Sun. The epoch of this figure shows the spacecraft passing behind the Sun as viewed from the Earth. The figure on the left shows the trajectory when the spacecraft would be within 10° of the Sun as viewed from the Earth. This period of 280 days will occur once every 3 years, provided the proper maneuvers are performed. Two similar periodic curves give the Sun-Earth-Probe angles for the two spacecraft while the lower smooth curve gives their angular separation as seen from the Earth.

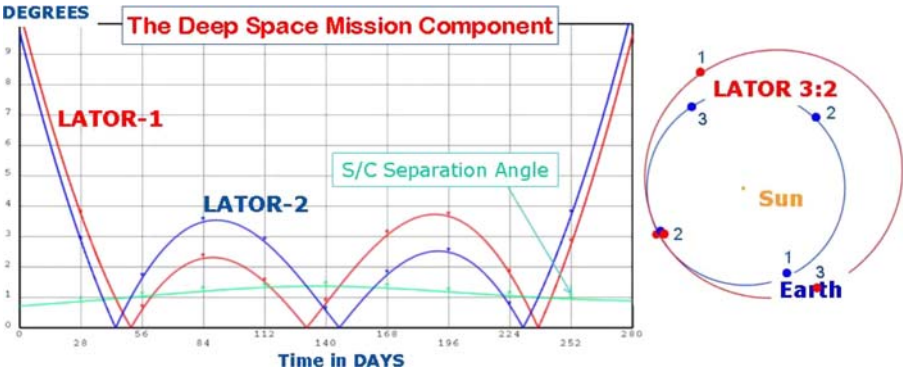

Fig. 5 *Left*: The Sun-Earth-Probe angle during the period of 3 occultations (two periodic curves) and the angular separation of the spacecraft as seen from the Earth (*lower smooth line*). Time shown is days from the moment when one of the spacecraft are at 10 distance from the Sun. *Right*: View from the North Ecliptic of the LATOR spacecraft in a 3:2 resonance. The epoch is taken near the first occultation

As a baseline design for the LATOR orbit, both spacecraft will be launched on the same launch vehicle. Almost immediately after the launch there will be a 30 m/s maneuver that separates the two spacecraft on their 3:2 Earth resonant orbits (see Fig. 5). The sequence of events that occurs during each observation period will be initiated at the beginning of each orbit of the ISS. It assumed that bore sighting of the spacecraft attitude with the spacecraft transmitters and receivers have already been accomplished. This sequence of operations is focused on establishing the ISS to spacecraft link. The interspacecraft link is assumed to be continuously established after deployment, since the spacecraft never lose line of sight with one another (for more details consult Section 5.4).

The 3:2 Earth resonant orbit provides an almost ideal trajectory for the LATOR mission, specifically i) it imposes no restrictions on the time of launch; ii) with a small propulsion maneuver after launch, it places the two LATOR spacecraft at the distance of less then 3.5° (or $\sim 14\ R\odot$) for the entire duration of the experiment (or ∼8 months); iii) it provides three solar conjunctions even during the nominal mission lifetime of 22 months, all within a 7 month period; iv) at a cost of an extra maneuver, it offers a possibility of achieving small orbital inclinations (to enable measurements at different solar latitudes); and, finally, v) it offers a very slow change in the Sun-Earth-Probe (SEP) angle of about $\sim R_{\odot}$ in 4 days. Furthermore, such an orbit provides three observing sessions during the initial 21 months after the launch, with the first session starting in 15 months [49]. As such, this orbit represents a very attractive choice for LATOR. We intend to further study this 3:2 Earth resonant trajectory as the baseline option for the mission.

4 LATOR interferometry

In this section, we describe the process of how the LATOR interferometer will be measuring angles. Since the spacecraft will carry lasers that are monochromatic sources, the interferometer can efficiently use heterodyne detection to measure the phase of the incoming signal. To this extent, we first present a simplified explanation of heterodyne interferometry proposed for the LATOR interferometer. We then describe the interferometric design of the LATOR station on the ISS.

4.1 Long-baseline optical interferometer on the ISS

The LATOR station on the ISS is used to interferometrically measure the angle between the two spacecraft and also to transmit and receive the laser ranging signals to each of the spacecraft. The station on the ISS is composed of a two laser beacon stations that perform communications and laser ranging to the spacecraft and two interferometer stations that collect the downlink signal for the astrometric measurement. This station also uses a fiber optic link to transmit the common local oscillator to the interferometer station.

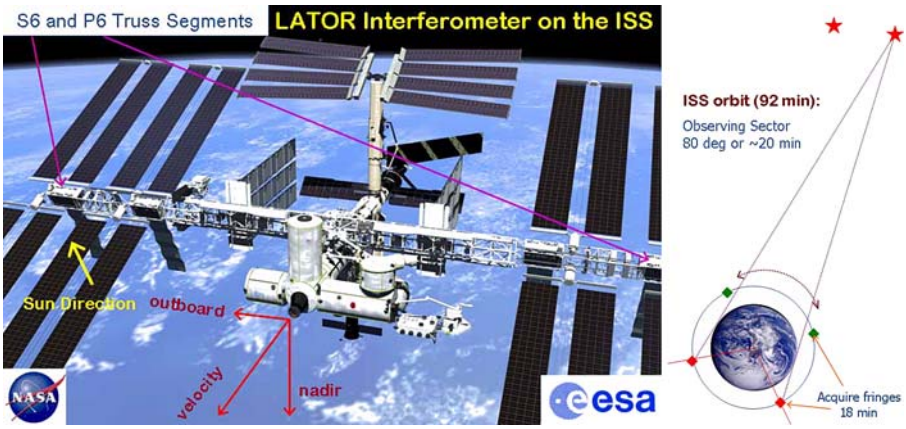

Fig. 6 *Left*: Location of the LATOR interferometer on the ISS. To utilize the inherent ISS Sun-tracking capability, the LATOR optical packages will be located on the outboard truss segments P6 and S6 outwards. *Right*: Signal acquisition for each orbit of the ISS. Note that variation of the baseline's projection allows to successfully solve the issue of the monochromatic fringe ambiguity

4.1.1 General description

The interferometer on the ISS will be formed by two optical packages (or laser beacon stations) with approximate dimensions of (0.6 m $\times$ 0.6 m $\times$ 0.6 m) for each package. The mass of each telescope assembly $\sim$120 kg. Both laser beacon stations must be physically located and integrated with the ISS infrastructure. Their location must provide a straight-line separation of $\sim$100 m between the two stations and have a clear line-of-sight (LOS) path between the two transceivers during the observation periods. Both packages must have clear LOS to both spacecraft during pre-defined measurement periods. Location on the ISS should maximize the inherent ISS sun-tracking capability. Both telescope assemblies will have to be able to point toward the Sun during each observing period which can be achieved by locating these payloads on the ISS outboard truss segments (P6 and S6 outward, see Fig. 6). A limited degree of automatic Sun-tracking capability is afforded by the α-gimbals on the ISS.

The minimum unobstructed LOS time duration between each transponder on the ISS and the transponders and their respective spacecraft will be 58 min per the 92 min orbit of the ISS. The pointing error of each transceivers to its corresponding spacecraft will be no greater than 1 μrad for control, 1 μrad for knowledge, with a stability of 0.1 μrad/s, provided by a combination of the standard GPS link available on the ISS and μ-g accelerometers.

4.1.2 Laser beacon station

The laser beacon stations provide the uplink signals to the LATOR spacecraft and detect their downlink signals. The transmitter laser signal is modulated for

laser ranging and to provide optical communications. Separate transmitters are used for each spacecraft each using a 1 W laser at 1064 nm as the source for each laser beacon. The laser beam is expanded to a diameter of 30 cm and is directed toward the spacecraft using a siderostat mirror. Fine pointing is accomplished with a fast steering mirror in the optical train.

During initial acquisition, the optical system of the laser beacon is modified to produce a beam with a 10 arcsec divergence. This angular spread is necessary to guarantee a link with the spacecraft, albeit a weak one, in the presence of pointing uncertainties. After the acquisition sequence is complete, the beam is narrowed to a diffraction limited beam, thereby increasing the signal strength.

The downlink laser signal at 1064 nm, is detected using a 12×12 (10×10 arcsec) array of Germanium detectors. In order to suppress the solar background, the signal is heterodyned with a local oscillator and detected within a narrow 1 MHz bandwidth. In the initial acquisition mode, the detection system searches over a 300 MHz bandwidth and uses a spiral search over a 30 arcsec angular field to find the downlink signal. Upon acquisition, the search bandwidth is decreased to 1 MHz and a quad-cell subarray is used to point the siderostat and fast steering mirrors of the beacon.

4.1.3 Interferometer station

The interferometer stations collect the laser signal from both spacecraft to perform the heterodyne measurements needed for the interferometric angle measurement. There are a total of five receivers to make the four angular measurements needed to resolve fringe ambiguity.

The detection and tracking system is basically similar to the receiver arm of the laser beacon described in the previous section. Light is collected by a 0.3 m siderostat mirror and compressed with a telescope to a manageable beam size. The light from each of the spacecraft is separated using a dual feed optical system. A fast steering mirror is used for high bandwidth pointing of the receiver. In addition a combination of a wideband interference filter and a narrow band Faraday Anomalous Dispersion Optical Filter (FADOF) will used to reject light outside a 0.05 nm band around the laser line. Each spacecraft signal is interfered with a local oscillator and the phase measurement time tagged and recorded. A 6×6 Ge array (5×5 arcsec FOV) is used to provide heterodyne acquisition and tracking of the LATOR spacecraft.

4.1.4 Interferometer on the ISS

Figure 7 shows a schematic of the ISS-based fiber interferometer that will be used to perform the angular measurement between the two LATOR spacecraft. The interferometer includes the heterodyne detection of the downlink signals that have been described in the previous section. The local oscillator (LO) is generated in one of the ground station receivers and is frequency locked to the laser signal from one of the spacecraft. The LO is then broadcast to the other station on the ISS through a 100 m single mode polarization

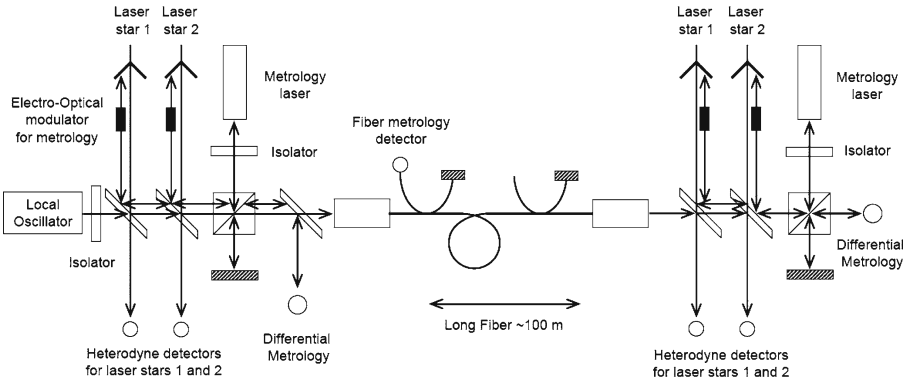

Fig. 7 Component description of the ISS-based interferometer

preserving fiber. The heterodyne signals from all the stations (2 stations, 2 signals each) are recorded and time tagged.

Figure 7 also shows two metrology systems used in the interferometer. The first metrology system measures the difference in optical path between the two laser signal paths and is essential to proper processing of the heterodyne data. The second metrology system measures the changes in the optical path through the fiber. This measurement monitors the length of the fiber and is used in the post processing of the interferometer data. The internal path metrology system, shown in the figure, measures the paths from corner cube on the siderostat mirror (shown as two, really only one) to the metrology beamsplitter. It is essential that the laser metrology system be boresighted to the laser signal path so the correct distance is measured. A Michelson interferometer with a frequency shift in one arm measures changes in the length of each signal path. Both spacecraft signal paths are measured simultaneously. This is accomplished by using an electro-optic cell and modulating each beam at a different frequency. A He–Ne laser is used as the light source for this metrology system. Filters at the output of the detector are then used to separate the signals corresponding to each metrology beam. The fiber metrology system measures changes in the optical path through the fiber.

4.2 Laser metrology transceiver subsystem

The metrology transceiver consists of the laser, frequency modulators, optics, and frequency stabilizer. The laser light is first frequency-stabilized to better than 1 part in 10^{10}, this is done in order to make the measurements. The laser light is then frequency-modulated in order to produce the heterodyne signal and distinguish between incoming and outgoing beams. Finally, light is collimated and injected into the beam launcher optics. The incoming metrology signal is received by the beam launcher optics and is interfered with the local

laser. A cat's eye retroreflector serves as the spacecraft fiducial and is common to all three beam launchers. Below we discuss these elements in more details.

4.2.1 Laser and frequency stabilization

A 1 W Nd:YAG laser operating at 1064 nm is used to transmit the metrology signals to the other spacecraft. The laser will be thermally tunable over a range of several GHz. Two lasers are used in each spacecraft for redundancy. The source laser is stabilized to 1 part in 10^{10} long term using a temperature controlled Fabry Perot etalon. A Pound-Drever scheme is used to servo the frequency of the laser to one of the longitudinal modes of the cavity. Control of the $\sim$3 cm cavity to 10 mK will achieve the required stability. Calibration of the cavity length on the ground will be done by injecting a second laser locked onto an adjacent longitudinal cavity mode and beating the two signals together. For the 3 cm cavity, the 5 GHz beat frequency must be known to 10^{-10}. Temperature control of the cavity will allow fine tuning of the laser frequencies between the spacecraft so that the heterodyne signal between two lasers lies below 2 MHz. This will require knowledge of the spacecraft relative velocity to 1 m/s, which is easily achievable.

4.2.2 Frequency modulators

The laser frequency is modulated in order to distinguish between the various transmit and receive beams used in the LATOR measurements. In addition, the relative velocity between the spacecraft can reach as high as 100 m/s. This will produce a Doppler frequency of up to 200 MHz between lasers from two spacecraft. The frequency of the modulator will be tuned to slightly offset from the Doppler frequency to minimize the bandwidth at which the data needs to be recorded.

Acousto-optic modulators (AOM) with fiber-coupled input and output are used. For a single metrology channel 3 different frequencies are needed for the reference, and two unknown signals. One implementation is a fiber-fed modulator which uses a bulk AOM and is insensitive to alignment errors. Other implementations for the AOMs will also be studied. These include integrated optic AOMs and multi-channel Bragg cells, both of which will be capable of generating the multiple signals at much lower mass. The metrology system will also need to phase lock the outgoing laser with the incoming laser. The AOM provides the phase modulation to the laser beam. The incoming signal and the laser output from the AOM are interfered on a high frequency detector. This signal is then used to servo the frequency of the AOM to null. This will produce a phase locked signal whose phase error is determined by the level of the null. In reality, because of the AOM, center frequency, the interfered signal will be upshifted by a stable local oscillator and the servoing done in RF. The stability of this local oscillator is the same as the required stability of the phase locked loop, 10^{-10}.

4.2.3 Beam launcher and receiver optics

In the current instrument design, the modulated laser beam is injected using a polarization preserving single mode fiber and expanded to a 0.5 cm beam. A cat's eye retroreflector is one of several devices that can be used as the metrology fiducial and is common to the three metrology beams. The cat's eye uses two optically contacted concentric hemispheres with radius of ∼10 cm and ∼20 cm. The cat's eye is sized many times larger than the beam in order to minimize the effect of spherical aberration.

The beam is then expanded to a 5 cm beam using a refractive telescope. A refractive design was chosen because changes in the optical path are relatively insensitive to changes in the position and orientation of the optical elements.

In order to measure the path length to better ∼ 5 pm, errors due to thermal effects on the beam launcher optics must be controlled. For example a change in the temperature of 1 mK on a 0.5 cm beamsplitter would produce a path length error of ∼ 5 pm; consequently an active thermal controller would be used on the beamsplitters, and telescope optics. Furthermore, baffles on the optics will be used to prevent external radiation from affecting the temperature of the instrument. The metrology optics will be mounted on a GrEp bench for thermal stability.

4.2.4 Acquisition camera and pointing subsystems

The acquisition camera will be used as the sensor for pointing the metrology beam. A 512 × 512 camera may be used to detect the position of the incoming laser beam to 0.5 arcsec over a 1° field by interpolating the centroid of the spot to 0.1 pixel. Three cameras will be used to track each of the incoming metrology beams. The outgoing laser beam will be retroreflected from the alignment corner cube to produce a spot on the acquisition camera on which to servo the pointing gimbal. The direction of the outgoing beam is set to the position of the target spacecraft, taking into account the point ahead angle. In the current instrument design the entire beam launcher optical assembly is gimbaled to point the metrology beam to the target spacecraft. The 2-axis gimbal has a center of rotation at the center of the cat's eye retro reflector. This optical arrangement measures the distance between the optical fiducials and is not sensitive to slight misalignments to the first order. The gimbal will have a range of 1° and a pointing resolution of 0.5 arcsec.

4.2.5 Laser ranging subsystem

The laser ranging system is used to determine the positions of the spacecraft with respect to the ISS. This is required to determine the impact parameter of the laser beam grazing the sun as well as the co-planarity of the three spacecraft. A time of flight laser ranging system is used to triangulate the spacecraft positions. A laser transponder system on the spacecraft is used to increase the SNR of the return pulse. Laser ranging will be performed with an

accuracy of ∼1 cm by integrating over a number of laser pulses. If the system were capable of instantaneously detecting delays of 100 ps (3 cm), at a 1 kHz repetition rate, it would take under 1 s to reach the desired accuracy. Assuming this level of ranging and using baseline 100 m will result in an accuracy in the transverse direction of 1 m at LATOR's orbit with spacecraft separated as much as 2 AU (see discussion of inter-spacecraft laser ranging operations in Section 5.1.2).

5 LATOR flight system

The LATOR flight system consists of two major components: the deep-space component that will be used to transmit and receive the laser signals needed to make science measurements and the interferometer on the ISS that will be used to interferometrically measure the angle between the two spacecraft and to transmit and receive the laser ranging signals to each of the spacecraft.

There are two LATOR spacecraft in the deep-space component of the mission, which will be used to transmit and receive the laser signals needed to make the science measurements. The flight system is subdivided into the instrument payload and a standard spacecraft bus. The instrument includes the laser ranging and communications hardware and is described in more detail in the following section. The spacecraft contains the remainder of the flight hardware which includes solar cells, attitude control, and the spacecraft structure.

5.1 LATOR instrument

The LATOR instrument in each of the two spacecraft consists of three laser metrology transmitters and receivers that can be gimbaled to point at the other spacecraft, and a camera system to acquire the incoming laser signals and to control the pointing of the outgoing beams. In addition, the instrument contains a laser ranging transponder in order to determine the spacecraft position from the ground. The LATOR instrument is used to perform laser ranging between the two spacecraft; it is also used (the second set) for laser ranging and optical communications between the spacecraft and the ISS.

5.1.1 ISS-to-spacecraft receiver and transmitter

The ISS-to-spacecraft receiver performs the acquisition, tracking, and detection of the signals from the ISS. This uplinked signal will be sent at 1064 nm and will contain modulation both to perform laser ranging and to send control signals to the spacecraft. The signals from the ISS are detected by a telescope with a collecting aperture of 20 cm. A coronograph will be used to suppress stray light from the Sun. In addition a combination of a wideband interference filter and a narrow band FADOF filter will used to reject light outside a 0.05 nm band around the laser line. The incoming signal is subdivided with

one portion going to a high bandwidth detector and the other to an acquisition and tracking CCD array. Using a 64×64 CCD array with pixels sized to a diffraction limited spot, this array will have a 5 arcmin field of view, which is greater than the pointing knowledge of the attitude control system and the point ahead angle (30 arcsec). After acquisition of the ISS beacon, a 2×2 element subarray of the CCD will be used as a quad cell to control the ISS–S/C two axis steering mirror. This pointing mirror is common to both the receiver and transmitter channel, to minimize misalignments between the two optical systems due to thermal variations. The pointing mirror will have 10 arcmin throw and a pointing accuracy of 0.5 arcsec, which will enable placement of the uplink signal on the high bandwidth detector.

The ISS-to-spacecraft transmitter sends a laser signal to both the interferometer collectors and the beacon receivers. The signal will be encoded for both ranging and communication information. In particular, the transmitted signal will include the inter-spacecraft ranging measurements. The transmitter uses a 1 W frequency stabilized Nd:YAG laser at 1064 nm. A 5 kHz line width is required to simplify heterodyne detection at the ground station. A 20 cm telescope is used to transmit the laser beam and a steering mirror is used for pointing. The mirror uses information from the attitude control system, the quad-cell detector in the receiver, and the point ahead information from the instrument controller to determine the transmit direction. A fast steering mirror is used to maintain high bandwidth pointing control for both the transmitter and receiver.

We have also considering the possibility of using a common optical system for both the transmitter and receiver. Because of the difference in the receive and transmit wavelengths, dichroic beam splitters and filters are used to minimize losses from the optics and leakage into the detectors. In this scheme a point-ahead mirror is used maintain a constant angular offset between the received and transmitted beams. Because of the common optical elements, this system is more tolerant to misalignments than the previous configuration.

5.1.2 Inter-spacecraft receiver and transmitter

The inter-spacecraft receiver/transmitter uses two separate optical systems. The receiver is similar in design to the ISS–Spacecraft receiver subsystem. Since there is no solar background contribution, the coronograph and FADOF filter have been removed. Detection of the signal is accomplished using a CCD for acquisition and a quad cell subarray for tracking. The tracking signal is also used to control the pointing of the transmitter minor. A separate high bandwidth detector is used for detecting the laser ranging signal.

The inter-spacecraft transmitter sends the laser ranging signal to the other spacecraft. The transmitter uses a 780 nm laser with an output power of 0.2 W (alternatively it may use a small fraction of the laser light that is used to establish spacecraft-to-ISS link). The transmitter and receiver telescopes have an aperture of 5 cm diameter. Because of the proximity of the LATOR spacecraft, thermal drifts that cause misalignments between the transmitter

and receiver optical systems can be sensed and corrected rapidly. In addition, the LATOR geometry requires minimal point-ahead, since the transverse velocity between spacecraft is nearly zero.

5.2 LATOR spacecraft

The LATOR spacecraft, like most spacecraft, will be composed of the following subsystems: thermal, structural, attitude control, power, command and data handling, telecommunications, and propulsion, that will be discussed below.

The basic thermal design will similar to that of the SA-200B, with modifications to account for the variation in range. This design uses basically passive thermal control elements with electric heaters/thermostats. The thermal control flight elements are multilayer insulation, thermal surfaces, thermal conduction control, and sensors. The active elements are minimized and will be only electric heaters/thermostats. To minimize heater power thermal louvers may be used. The current design assumes that the spacecraft uses passive thermal control with heaters/thermostats, because it is basically designed for Earth orbit.

The current best estimate for the total dry mass is 115 kg including a set of required modifications to the standard SA-200B bus (i.e., a small propulsion system, a 0.5 m HGA for deep-space telecom, etc.) The design calls for launching the two spacecraft on a custom carrier structure, as they should easily fit into the fairing. The total launch mass for the two spacecraft will be 552 kg.

An attitude control system may be required to have pointing accuracy of 6 μrad and a pointing knowledge of 3 μrad. This may be achieved using a star tracker and sun sensor combination to determine attitude together with reaction wheels (RW) to control attitude. Cold-gas jets may be used to desaturate RWs. For the current experiment design it is sufficient to utilize a pointing architecture with the following performance (3σ, per axis): control 6 μrad; knowledge 3 μrad; stability 0.1 μrad/s. The SA-200B readily accommodates these requirements.

The flight system will require ∼50 W of power. This may be supplied by a 1 square meter GaAs solar cell array. To maintain a constant attitude with respect to the Sun, the solar cells must be deployed away from the body of the spacecraft. This will allow the cells to radiate away its heat to maintain the cells within their operating temperature range.

The telecommunications subsystem will be a hybrid that utilizes the optical communications capability of the instrument as the primary means of transmitting and receiving commands and data. In addition, a small low gain antenna for low data rate radio communications will be used for emergency purposes. This system will use a 15 W transmitter and 10 dB gain antenna. Using X band this system can operate with a 5 bit per second (bps) data rate. The design calls for an SDST X-Band transponder, operating at 15 W; X-Band SSPA; a 0.5 m HGA; two X-Band LGAs pointed opposite each other;

a duplexer; two switches; and coax cabling—the standard options of present day spacecraft design.

The propulsion subsystem for SA-200S bus may be used as is. This will ensure a minimal amount of engineering is required. The system is a blowdown monopropellant system with eight 5-N thrusters and two 32 cm tanks each with 22 kg propellant capacity. The system exists and was tested in many applications.

We shall now consider the basic elements of the LATOR optical receiver system. While we focus on the optics for the two spacecraft, the interferometer has essentially similar optical architecture.

5.3 Optical receiver system

The LATOR 200 mm receiver optical system is a part of a proposed experiment. This system is located at each of two separate spacecraft placed on heliocentric orbits. The receiver optical system captures optical communication signals form a transmitter on the ISS, which orbits the Earth. To support the primary mission objective, this system must be able to receive the optical communication signal from the uplink system at the ISS that passes through the solar corona at the immediate proximity of the solar limb (at a distance of no more than 5 Airy disks).

Our recent analysis of the LATOR receiver optical system successfully satisfied all the configuration and performance requirements [40, 50, 51]. We have also performed a conceptual design, which was validated with a ray-trace analysis. The ray-trace performance of the designed instrument is diffraction limited in both the APD and CCD channels over the specified field of view at 1064 nm. The design incorporated the required field stop and Layot stop. A preliminary baffle design has been developed for controlling the stray light.

The out-of-field solar radiation falls on the narrow band pass filter and primary mirror; the scattering from these optical surfaces puts some solar radiation into the FOV of the two focal planes. This imposes some requirements on the instrument design. Thus, the narrow band pass filter and primary mirror optical surfaces must be optically smooth to minimize narrow angle scattering. This may be difficult for the relatively steep parabolic aspheric primary mirror surface. However, the field stop will eliminate direct out-of-field solar radiation at the two focal planes, but it will not eliminate narrow angle scattering for the filter and primary mirror. Finally, the Lyot stop will eliminate out-of-field diffracted solar radiation at the two focal planes. Additional baffle vanes may be needed at several places in the optical system.

5.4 LATOR observing sequence

It is important to discuss the sequence of events that will lead to the signal acquisition and that occur during each observation period (i.e., every orbit of the ISS). This sequence will be initiated at the beginning of the experiment period, after ISS emergence from the Earth's shadow (see Fig. 6). It assumes

that boresighting of the spacecraft attitude with the spacecraft transmitters and receivers have already been accomplished. This sequence of operations is focused on establishing the ISS to spacecraft link. The interspacecraft link is assumed to be continuously established after final deployment (at $\sim 15^\circ$ off the Sun), since the spacecraft never lose line of sight with one another.

The laser beacon transmitter at the ISS is expanded to have a beam divergence of 10 arcsec in order to guarantee illumination of the LATOR spacecraft. After re-emerging from the Earth's shadow this beam is transmitted to the craft and reaches them in about 18 minutes. At this point, the LATOR spacecraft acquire the expanded laser beacon signal. In this mode, a signal-to-noise ratio (SNR) of 23.2 can be achieved with 60 s of integration. With an attitude knowledge of 10 arcsec and an array field of view of 30 arcsec no spiral search is necessary. Upon signal acquisition, the receiver mirror on the spacecraft will center the signal and use only the center quad array for pointing control. Transition from acquisition to tracking should take about 1 min. Because of the weak uplink intensity, at this point, tracking of the

Table 3 Analysis of various links between ISS and spacecraft in observation and acquisition modes

Optical link parameters	Spacecraft-to-ISS link spacecraft=Xmit, ISS=Rcv		ISS-to-Spacecraft link ISS=Xmit, spacecraft=Rcv	
	Acquisition	Observation	Acquisition	Observation
Transmitter parameters				
Laser power, W	1	1	1	1
Wavelength, μm	1.064	1.064	1.064	1.064
Xmit telescope diameter, m	0.2	0.2	0.3	0.3
Beam divergence, μrad	10 asec	5.32	10 asec	3.55
Distance ($L = 2$ AU), m	3.00×10^{11}	3.00×10^{11}	3.00×10^{11}	3.00×10^{11}
Footprint diameter at L, m	1.45×10^{7}	1.59×10^{6}	1.45×10^{7}	1.06×10^{6}
Optics efficiency	0.7	0.7	0.7	0.7
Pointing efficiency	0.9	0.9	0.9	0.9
Receiver parameters				
Rcv telescope diameter, m	0.3	0.3	0.2	0.2
Rcv optics efficiency	0.7	0.7	0.7	0.7
Detector quantum efficiency	0.9	0.9	0.9	0.9
Power received, W	1.70×10^{-16}	1.41×10^{-14}	7.55×10^{-17}	1.41×10^{-14}
Photon flux received, ph/s	9.10×10^{2}	7.55×10^{4}	4.04×10^{2}	7.55×10^{4}
Solar background parameters				
Solar irradiance, ph/s/m^2/sr/μm	4.64×10^{25}	4.64×10^{25}	4.64×10^{25}	4.64×10^{25}
Rcv detector size, μrad	3.55	3.55	5.32	5.32
Heterodyne spectral bandwidth	300 MHz	1 MHz	–	–
Narrow-bandpass filter, μm	–	–	5×10^{-5}	5×10^{-5}
Coronograph efficiency	1×10^{-5}	1×10^{-5}	1×10^{-5}	1×10^{-5}
Solar photon flux received, ph/s	2.95×10^{2}	9.82×10^{-1}	1.30×10^{4}	1.30×10^{4}
Signal to noise ratio				
Integration time	1 s	10 ms	60 s	10 ms

ISS station is done at a very low bandwidth. The pointing information is fed-forward to the spacecraft transmitter pointing system and the transmitter is turned on. The signal is then re-transmitted down to the ISS with a light-travel time of 18 min.

Each interferometer station and laser beacon station searches for the spacecraft laser signal. In acquisition mode, the return is heterodyned by using an expanded bandwidth of 300 MHz, to assure capture of the laser frequency (Table 3). In this case, the solar background is the dominant source of noise, and an SNR of 22.5 is achieved with 1 s integration. Because of the small field of view of the array, a spiral search will take 30 s to cover a 30 arcsec field. Upon acquisition, the signal will be centered on the quad cell portion of the array and the local oscillator frequency locked to the spacecraft signal. The frequency band will then be narrowed to 1 MHz and the local oscillator frequency locked to the download laser. In this regime, the solar background is no longer the dominant noise source and an SNR of 24.7 can be achieved in only 10 ms of integration. The laser beacon transmitter will then narrow its beam to be diffraction limited ($\sim$1 arcsec) and to point toward the LATOR spacecraft. This completes the signal acquisition phase, and the entire architecture is in-lock and transmits scientific signal. This procedure is re-established during each 92-min orbit of the ISS.

5.5 Factors affecting SNR analysis

In conducting the signal-to-noise analysis we pay significant attention to several important factors. In particular, we estimate what fraction of the transmitted signal power captured by the 20 cm receiver aperture and analyze the effect of the Gaussian beam divergence (estimated at ~ 7 μrad) of the 30 cm transmit aperture on the ISS. Given the fact that the distance between the transmitter and receiver is on the order of 2 AU, the amount captured is about 2.3×10^{-10} of the transmitted power.

We also consider the amount of solar disk radiation scattered into the two receiver focal planes. In particular, the surface contamination, coating defects, optical roughness and substrate defects could scatter as much as 1×10^{-4} or more (possibly 1×10^{-3}) of the solar energy incident on the receive aperture into the field of view. These issues are being considered in our current analysis. We also study the amount of the solar corona spectrum within the receive field of view that is not blocked by the narrow band pass filter. The factors we consider is the filter's FWHM band-pass is 0.05 nm, the filter will have 4.0 optical density blocking outside the 0.05 nm filter band pass from the X-ray region of 1200 nm; the filter efficiency within the band pass will be about 35%, and the detector is probably sensitive from 300 nm to 1200 nm.

Additionally, we consider the amount of out-of-field solar radiation scattered into the focal plane by the optical housing. This issue needs to be investigated in a stray light analysis which can be used to optimize the baffle design to minimize the stray light at the focal plane. Finally, we study the effectiveness of the baffle design in suppressing stray light at the focal plane.

Thus, in addition to the stray light analysis, the effectiveness of the final baffle design should be verified by building an engineering model that can be tested for stray light.

Our recent conceptual design met all the configuration and performance requirements. In the near future, we plan to perform a stray light analysis which should be performed to optimize the baffle design and calculate the amount of stray light that could be present at each of the two focal planes. This stray light analysis will take into account the optical smoothness of the band-pass filter and primary mirror surfaces. Narrow angle scattering may be a problem at the two focal planes in the filter and primary mirror are not optically very smooth and, thus, it requires a more detailed study. Finally, a rigorous signal-to-noise analysis will be performed to validate the power required to achieve a high signal-to-noise ratio in detecting received beam signal in the presence of the expected focal beam stray light predicted by the stray light analysis and the engineering model stray light tests.

6 Discussion

The LATOR mission aims to carry out a test of the curvature of the solar system's gravity field with an accuracy better than 1 part in 10^9. In spite of previous space missions exploiting radio waves for tracking the spacecraft, this mission manifests an actual breakthrough in the relativistic gravity experiments as it allow one to take full advantage of the optical techniques that recently became available. LATOR benefits from a number of advantages over techniques that use radio waves to study the light propagation in the solar vicinity. The use of monochromatic light enables the observation of the spacecraft almost at the limb of the Sun, as seen from the ISS. The use of narrowband filters, coronagraph optics, and heterodyne detection will suppress background light to a level where the solar background is no longer the dominant noise source. The short wavelength allows much more efficient links with smaller apertures, thereby eliminating the need for a deployable antenna. Advances in optical communications technology allow low bandwidth telecommunications with the LATOR spacecraft without having to deploy high gain radio antennae needed to communicate through the solar corona. Finally, the use of the ISS not only makes the test affordable, but also allows conducting the experiment above the Earth's atmosphere—the major source of astrometric noise for any ground based interferometer. This fact justifies the placement of LATOR's interferometer node in space.

The concept is technologically sound; the required technologies have been demonstrated as part of the international laser ranging activities and optical interferometry programs at JPL. LATOR uses geometric redundancy of the optical truss to achieve a very precise determination of the interplanetary distances between the two micro-spacecraft and a beacon station on the ISS. The experiment takes advantage of the existing space-qualified optical technologies, leading to an outstanding performance in a reasonable mission

development time. In addition, the issues of the extended structure vibrations on the ISS, interferometric fringe ambiguity, and signal acquisition on the solar backgrounds have all been analyzed, and do not compromise mission goals. The ISS is the default location for the interferometer, however, ground- and free-flying versions have also been studied. While offering programmatic benefits, these options differ in cost, reliability and performance. The availability of the ISS makes presented concept realizable in the near future.

LATOR is envisaged as a partnership between NASA and ESA wherein both partners are essentially equal contributors, while focusing on different mission elements: NASA provides the deep space mission components and interferometer design, while building and servicing infrastructure on the ISS is an ESA contribution. The NASA focus is on mission management, system engineering, software management, integration, the launch vehicle for the deep space component, and operations. The European focus is on interferometer components, the initial payload integration, optical assemblies and testing of the optics in a realistic ISS environment. The proposed arrangement would provide clean interfaces between familiar mission elements.

This mission may become a 21st century version of the Michelson-Morley experiment in the search for a cosmologically evolved scalar field in the solar system. As such, LATOR will lead to very robust advances in the tests of fundamental physics: it could discover a violation or extension of general relativity, and/or reveal the presence of an additional long range interaction in the physical law. With this mission testing theory to several orders of magnitude higher precision, finding a violation of general relativity or discovering a new long range interaction could be one of this era's primary steps forward in fundamental physics. There are no analogs to the LATOR experiment; it is unique and is a natural culmination of solar system gravity experiments.

Acknowledgements The work described here was carried out at the Jet Propulsion Laboratory, California Institute of Technology, under a contract with the National Aeronautics and Space Administration.

References

1. Anderson, J.D., Williams, J.G.: Long-range tests of the equivalence principle. Class. Quantum Gravity **18**, 2447 (2001)
2. Anderson, J.D., Lau, E.L., Turyshev, S.G., Williams, J.G., Nieto, M.M.: Recent results for solar-system tests of general relativity. BAAS **34**, 833 (2002)
3. Bean, R., Carroll, S.M., Trodden, M.: Insights into dark energy: interplay between theory and observation (2005). astro-ph/0510059
4. Bennett, C.L., Halpern, M., Hinshaw, G., Jarosik, N., Kogut, A., Limon, M., Meyer, S.S., Page, L., Spergel, D.N., Tucker, G.S., Wollack, E., Wright, E.L., Barnes, C., Greason, M.R., Hill, R.S., Komatsu, E., Nolta, M.R., Odegard, N., Peirs, H.V., Verde, L., Weiland, J.L., [i.e. WMAP Science Team]: First year Wilkinson Microwave Anisotropy Probe (WMAP) observations: preliminary maps and basic results. Astrophys. J. Suppl. **148**, 1 (2003). astro-ph/0302207

5. Bertolami, O., Páramos, J.: The pioneer anomaly in the context of the braneworld scenario. Class. Quantum Gravity **21**, 3309 (2004) gr-qc/0310101
6. Bertolami, O., Páramos, J.: Astrophysical constraints on scalar field models. Phys. Rev. **D71**, 023521 (2004). astro-ph/0408216
7. Bertolami, O., Páramos, J., Turyshev, S.G.: General theory of relativity: will it survive the next decade? In: Proc. 359th WE-Heraeus Seminar: Lasers, Clock, and Drag-free: Technologies for Future Exploration in Space and Gravity Tests. University of Bremen, ZARM, Bremen, Germany, 30 May–1 June 2005. "Lasers, Clocks, and Drag-Free: Exploration of Relativistic Gravity in Space." H. Dittus, C. Laemmerzahl, S. Turyshev, editors. (Springer Verlag, 2006), pp. 27-67 (2006), gr-qc/0602016
8. Bertotti, B., Iess, L., Tortora, P.: A test of general relativity using radio links with the Cassini spacecraft. Nature **425**, 374 (2003)
9. de Bernardis, P., Ade, P.A.R., Bock, J.J., Bond, J.R., Borrill, J., Boscaleri, A., Coble, K., Crill, B.P., De Gasperis, G., Farese, P.C., Ferreira, P.G., Ganga, K., Giacometti, M., Hivon, E., Hristov, V.V., Iacoangeli, A., Jaffe, A.H., Lange, A.E., Martinis, L., Masi, S., Mason, P.V., Mauskopf, P.D., Melchiorri, A., Miglio, L., Montroy, T., Netterfield, C.B., Pascale, E., Piacentini, F., Pogosyan, D., Prunet, S., Rao, S., Romeo, G., Ruhl, J.E., Scaramuzzi, F., Sforna, D., Vittorio, N.: A flat universe from high-resolution maps of the cosmic microwave background radiation. Nature **404**, 955 (2000)
10. Capozziello, S., Troisi, A.: PPN-limit of fourth order gravity inspired by scalar-tensor gravity. Phys. Rev. **D72**, 044022 (2005). astro-ph/0507545
11. Carroll S.M.: The cosmological constant. Living Rev. Rel. **4**, 1 (2001). astro-ph/0004075
12. Carroll, S.M., Hoffman, M., Trodden, M.: Can the dark energy equation-of-state parameter w be less than -1? Phys. Rev. **D68**, 023509 (2003). astro-ph/0301273
13. Carroll, S.M., Duvvuri, V., Trodden, M., Turner, M.: Is cosmic speed-up due to new gravitational physics? Phys. Rev. **D70**, 043528 (2004). astro-ph/0306438
14. Carroll, S.M., De Felice, A., Duvvuri, V., Easson, D.A., Trodden, M., Turner M.S.: The cosmology of generalized modified gravity models (2005). astro-ph/0410031
15. Carroll, S.M.: Is our universe natural? (2005). hep-th/0512148
16. Damour, T., Nordtvedt, K.L., Jr.: General relativity as a cosmological attractor of tensor scalar theories. Phys. Rev. Lett. **70**, 2217 (1993)
17. Damour, T., Nordtvedt, K.L., Jr.: Tensor-scalar cosmological models and their relaxation toward general relativity. Phys. Rev. **D48**, 3436 (1993)
18. Damour, T., Polyakov, A.M.: String theory and gravity. Gen. Relativ. Gravit. **26**, 1171 (1994)
19. Damour, T., Polyakov, A.M.: The string dilaton and a least coupling principle. Nucl. Phys. **B423**, 532 (1994)
20. Damour, T., Esposito-Farese, G.: Testing gravity to second post-Newtonian order: a field-theory approach. Phys. Rev. **D53**, 5541 (1996a). gr-qc/9506063
21. Damour, T., Esposito-Farese, G.: Tensor-scalar gravity and binary pulsar experiments. Phys. Rev. **D54**, 1474 (1996b). gr-qc/9602056
22. Damour, T., Esposito-Farese, G.: Gravitational-wave versus binary-pulsar tests of strong-field gravity. Phys. Rev. **D58**, 042001 (1998). gr-qc/9803031
23. Damour T., Taylor J.H.: Strong-field tests of relativistic gravity and binary pulsars. Phys. Rev. **D45**, 1840 (1992)
24. Damour, T., Piazza, F., Veneziano, G.: Runaway dilaton and equivalence principle violations. Phys. Rev. Lett. **89**, 081601 (2002). gr-qc/0204094
25. Damour, T., Piazza, F., Veneziano, G.: Violations of the equivalence principle in a dilaton-runaway scenario. Phys. Rev. **D66**, 046007 (2002). hep-th/0205111
26. Dvali, G., Gabadadze, G., Porrati, M.: 4D gravity on a brane in 5D Minkowski space. Phys. Lett. **B485**, 208 (2000). hep-th/0005016
27. Dvali, G., Gabadadze, G., Porrati, M.: On sub-millimeter forces from extra dimensions. Mod. Phys. Lett. **A15**, 1717 (2000). hep-ph/0007211
28. Dvali, G., Gruzinov, A., Zaldarriaga, M.: The accelerated universe and the moon. Phys. Rev. **D68**, 024012 (2003). hep-ph/0212069
29. Halverson, N.W., Leitch E.M., Pryke C., Kovac, J., Carlstrom, J.E., Holzapfel, W.L., Dragovan, M., Cartwright, J.K., Mason, B.S., Padin, S., Pearson, T.J., Shepherd, M.C., Readhead,

A.C.S.: DASI first results: a measurement of the cosmic microwave background angular power spectrum. Astrophys. J. **568**, 38 (2002). astro-ph/0104489
30. Lange, Ch., Camilo, F., Wex, N., Kramer, M., Backer, D.C., Lyne, A.G. Doroshenko, O.: Precision timing measurements of PSR J1012+5307. Mon. Not. R. Astron. Soc. **326**, 274 (2001)
31. Lebach, D.E., Corey, B.E., Shapiro, I.I., Ratner, M.I., Webber, J.C., Rogers, A.E.E., Davis, J.L. Herring, T.A.: Measurement of the solar gravitational deflection of radio waves using very-long-baseline interferometry. Phys. Rev. Lett. **75**, 1439 (1995)
32. Netterfield, C.B., Ade, P.A.R., Bock, J.J., Bond, J.R., Borrill, J., Boscaleri, A., Coble, K., Contaldi, C.R., Crill, B.P., de Bernardis, P., Farese, P., Ganga, K., Giacometti, M., Hivon, E., Hristov, V.V., Iacoangeli, A., Jaffe, A.H., Jones, W.C., Lange, A.E., Martinis, L., Masi, S., Mason, P., Mauskopf, P.D., Melchiorri, A., Montroy, T., Pascale, E., Piacentini, F., Pogosyan, D., Pongetti, F., Prunet, S., Romeo, G., Ruhl, J.E., Scaramuzzi, F. [i.e. Boomerang Collaboration]: A measurement by BOOMERANG of multiple peaks in the angular power spectrum of the cosmic microwave background. Astrophys. J. **571**, 604 (2002). astro-ph/0104460
33. Nordtvedt, K.L., Jr.: Probing gravity to the 2nd post-Newtonian order and to one part in 10^7 using the Sun. ApJ **320**, 871 (1987)
34. Nordtvedt, K.L., Jr.: Significance of 'second-order' light propagation experiments in the solar system. Class. Quantum Gravity **13**, A11 (1996)
35. Nordtvedt, K.L., Jr.: Lunar laser ranging—a comprehensive probe of post-Newtonian gravity (2003). gr-qc/0301024
36. Peebles, P.J.E., Ratra, B.: The cosmological constant and dark energy. Rev. Mod. Phys. **75**, 599 (2003). astro-ph/0207347
37. Peacock, J.A., et al.: A measurement of the cosmological mass density from clustering in the 2dF galaxy redshift survey. Nature **410**, 169 (2001)
38. Perlmutter, S., Aldering, G., Goldhaber, G., Knop, R.A., Nugent, P., Castro, P.G., Deustua, S., Fabbro, S., Goobar, A., Groom, D.E., Hook, I.M., Kim, A.G., Kim, M.Y., Lee, J.C., Nunes, N.J., Pain, R., Pennypacker, C.R., Quimby, R., Lidman, C., Ellis, R.S., Irwin, M., McMahon, R.G., Ruiz-Lapuente, P., Walton, N., Schaefer, B., Boyle, B.J., Filippenko, A.V., Matheson, T., Fruchter, A.S., Panagia, N., Newberg, H.J.M., Couch, W.J. [i.e. Supernova Cosmology Project Collaboration]: Measurements of omega and lambda from 42 high-redshift supernovae. Astrophys. J. **517**, 565 (1999). astro-ph/9812133
39. Pitjeva, E.V.: Relativistic effects and solar oblateness from radar observations of planets and spacecraft. Astron. Lett. **31**, 340 (2005)
40. Plowman, J.E., Hellings, R.W.: LATOR covariance analysis. Class. Quantum Gravavity **23**, 309 (2006). gr-qc/0505064
41. Reasenberg, R.D., Shapiro, I.I., MacNeil, P.E., Goldstein, R.B., Breidenthal, J.C., Brenkle, J.P., Cain, D.L., Kaufman, T.M., Komarek, T.A., Zygielbaum, A.I.: Viking relativity experiment: verification of signal retardation by solar gravity. ApJ Lett. **234**, L219 (1979)
42. Robertson, D.S., Carter, W.E., Dillinger, W.H.: A new measurement of solar gravitational deflection of radio signals using VLBI. Nature **349**, 768 (1991)
43. Riess, A.G., Filippenko, A.V., Challis, P., Clocchiatti, A., Diercks, A., Garnavich, P.M., Gilliland, R.L., Hogan, C.J., Jha, S., Kirshner, R., Leibundgut, B., Phillips, M.M., Reiss, D., Schmidt, B.P., Schommer, R.A., Smith, R.C., Spyromilio, J., Stubbs, C., Suntzeff, N.B., Tonry, J.: Observational evidence from supernovae for an accelerating universe and a cosmological constant. [i.e., Supernova Search Team Collaboration] Astron. J. **116**, 1009 (1998)
44. Shapiro, I.I., Counselman, C.C., III, King, R.W.: Verification of the principle of equivalence for massive bodies. Phys. Rev. Lett. **36**, 555 (1976)
45. Shapiro, I.I., Reasenberg, R.D., MacNeil, P.E., Goldstein, R.B., Brenkle, J.P., Cain, D.L., Komarek, T., Zygielbaum, A.I., Cuddihy, W.F., Michael, W.H., Jr.: The viking relativity experiment. JGR **82**, 4329 (1977)
46. Shapiro, S.S., Davis, J.L., Lebach, D.E., Gregory, J.S.: Measurement of the solar gravitational deflection of radioWaves using geodetic very-long-baseline interferometry data, 1979–1999. Phys. Rev. Lett. **92**, 121101 (2004)
47. Taylor, J.H., Wolszczan, A., Damour, T., Weisberg, J.M.: Experimental constraints on strong-field relativistic gravity. Nature **355**, 132 (1992)
48. Tonry, J.L., Schmidt, B.P., Barris, B., Candia, P., Challis, P., Clocchiatti, A., Coil, A.L., Filippenko, A.V., Garnavich, P., Hogan, C., Holland, S.T., Jha, S., Kirshner, R.P., Krisciunas,

K., Leibundgut, B., Li, W., Matheson, T., Phillips, M.M., Riess, A.D., Schommer, R., Smith, R.C., Sollerman, J., Spyromilio, J., Stubbs, C.W., Suntzeff, N.B.: Cosmological results from high-z supernovae. Astrophys. J. **594**, 1–24 (2003). astro-ph/0305008
49. Turyshev, S.G., Shao, M., Nordtvedt, K.L., Jr.: The Laser Astrometric Test of Relativity (LATOR) mission. Class. Quantum Gravity **21**, 2773 (2004). gr-qc/0311020
50. Turyshev, S.G., Shao, M., Nordtvedt, K.L., Jr.: Experimental design for the LATOR mission. Int. J. Mod. Phys. **D13**, 2035 (2004). gr-qc/0410044
51. Turyshev, S.G., Shao, M., Nordtvedt, K.L., Jr.: Optical design for the Laser Astrometric Test of Relativity. In: Proc. The XXII Texas Symposium on Relativistic Astrophysics. Stanford University, 13–17 December 2004, eConf C041213 #0306 (2004). gr-qc/0502113
52. Turyshev, S.G., Shao, M., Nordtvedt, K.L., Jr.: Science, technology and mission design for the Laser Astrometric Test of Relativity mission. 359th WE-heraeus Seminar: Lasers, Clock, and Drag-free: Technologies for Future Exploration in Space and Gravity Tests. University of Bremen, ZARM, Bremen, Germany, 30 May–1 June 2005. In: Dittus, H., Laemmerzahl, C., Turyshev, S. (eds.) Lasers, Clocks, and Drag-free: Technologies for Future Exploration in Space and Tests of Gravity: Proceedings, pp. 429-493. Springer Verlag (2006). arXiv:gr-qc/0601035
53. Turyshev, S.G., Israelsson, U.E., Shao, M., Yu, N., Kusenko, A., Wright, E.L., Everitt, C.W.F., Kasevich, M., Lipa, J.A., Mester, J.C., Reasenberg, R.D., Walsworth, R.L., Ashby, N., Gould, H., Paik, H.J.: Space-based research in fundamental physics and quantum technologies. Int. J. Mod. Phys. D **16**(12a), 1879–1925 (2007). arXiv:0711.0150 [gr-qc]
54. Turyshev S. G.: Experimental tests of general relativity. Annu. Rev. Nucl. Part. Sci. **58**, 207–248 (2008). arXiv:0806.1731 [gr-qc]
55. Will, C.M.: Theory and experiment in gravitational physics. Cambridge: Cambridge University Press (1993)
56. Will, C.M.: The confrontation between general relativity and experiment. Liv. Rev. Relativity **9** (2006). gr-qc/0510072
57. Williams, J.G., Turyshev, S.G., Boggs, D.H.: Progress in lunar laser ranging tests of relativistic gravity. Phys. Rev. Lett. **93**, 261101 (2004) gr-qc/0411113